SEMARAK ILMU PUBLISHING

Journal of Advanced Research in Fluid Mechanics and Thermal Sciences

Journal homepage:
https://semarakilmu.com.my/journals/index.php/fluid_mechanics_thermal_sciences/index
ISSN: 2289-7879

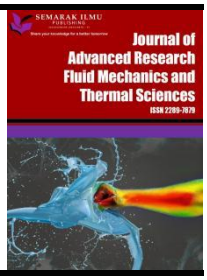

A Model on Free Convective Casson Fluid Flow Past a Permeable Vertical Plate with Gyrotactic Microorganisms

Abubakar Usman[1,*], Siti Sabariah Abas[1], Nurul Aini Jaafar[2], Muhammad Hassan Muhammad[1], Mustafa Mamat[1]

[1] Faculty of Informatics & Computing, Universiti Sultan Zainal Abidin, 22200 Besut, Terengganu, Malaysia
[2] Department of Mathematical Sciences, Faculty of Science, Universiti Teknologi Malaysia, 81310, Skudai, Johor Bahru, Malaysia

ARTICLE INFO

Article history:
Received 3 January 2023
Received in revised form 4 April 2023
Accepted 10 April 2023
Available online 27 April 2023

Keywords:
Gyrotactic microogranisms; Casson fluid; Soret-Dufour; spectral relaxation technique; free convective

ABSTRACT

This study focused on free convective MHD Casson fluid flow past a permeable vertical plate with microorganisms and Soret-Dufour mechanisms. The physical model is governed by system of partial differential equations (PDEs). The set of PDEs were overhaul into a nonlinear ordinary differential equation by considering acceptable similarity variable. The spectral relaxation method (SRM) was utilized to obtain solution to the overhaul nonlinear ordinary differential equations. This study examined critically the significant of the Gyrotactic microorganisms on Casson fluid locomotion Also, the significance of parameters such as thermal radiation, Soret-Dufour mechanisms, Brownian motion, Joule heating and so on are examined on velocity, concentration, motile microorganism and temperature profiles. The Casson parameter was found to intensify the velocity contour and the hydrodynamic boundary layer thickness. A higher magnetic parameter gives rise to Lorentz force which declines the motion of the fluid. There is higher temperature within the boundary layer because of the presence of thermal radiation.

1. Introduction

The studies of bioconvection over external flows in micro-organism mediated devices are receiving growing attention in many research and industrial quarters. Particularly, emerging technology in biofuel, immunology and tissue engineering that require bioreactor for processing of activities of motile microorganisms is strengthen research and industrial endeavour in the subject area. The development of complex bioartificial systems such as liver and pancreas could be implemented on slender-membered membranes bioreactors because of its capacity to limit the incidence of fouling in the reaction chamber during sensitive bioprocesses. Maschhoff *et al.,* [1], while bioconvection is associated with the dynamics of microbial-constituents in a fluid media, one could justify the fundamental role of fluid mechanics in delineating and predicting transport within this domain. It is obvious; the presence of thin-sized slender shape membrane and stirrer

* *Corresponding author.*
E-mail address: abubakarusman847@gmail.com

https://doi.org/10.37934/arfmts.105.2.3150

components in bioreactor assembly interfacing the microorganism models a typical scenario in hydrodynamics. Ahmed *et al.,* [2] examined the mechanisms of Soret-Dufour, MHD, heat along with mass transfer together with buoyancy force as well as viscous dissipation influence. Hence, the scrutiny of fluid transport, and associated reaction dynamics in the near-field of bioreactor members that are defined with slender configurations may be bequeathed to fluid mechanist.

The nanofluid contains nano meter-sized particles. It is called nanoparticles. The study of nanofluid can be homogeneous and two-phase methods. Many things have been explored on the influence of thermal conductivity on nanofluids. The most important aspect of nanofluid is its size and temperature. The nanofluid has large colloidal suspension stability and it is important in heat transfer along with transport properties when its size, shape, concentration along particle material is altered. The nanoparticles have both biomedical and environmental applications. The environmental applications find usefulness in water treatment, bioremediation of diverse contaminants and in the production of clean energy while the biomedical applications are basically the imaging, biosensing as well as drug delivery. The consequences of thermophoresis on nanoparticle dissemination have been investigated by Bahiraei [3]. It was discovered that the incorporation of huge particles gives variation in concentration dissemination. Seferis *et al.,* [4] analyzed Grain's size along with the outline reliance of luminescence productivity. The sedimentation approach was utilized and the rod analogous grain screens show together with a reduced efficiency of luminescence. Abdollahi *et al.,* [5] elucidate the heat movement of nanofluids situated in a microchannel. It was finalized in their paper that higher infraction of nanoparticles volume along with a degeneration in the diameter of nanoparticle elevates the value of Nusselt number. Ahmed and Rashed [6] studied MHD heat generating penetrable region filled wavy enclosures. They applied Buongiorno's nanofluid concept to the creation of heat in a permeable channel. It has been explained that Hartmann number growth obstructs fluid mobility while increasing the rate of heat transfer. Convection on micro along with nanoliquids with Cattaneo-Christov heat flux has been studied by Upadhya *et al.,* [7]. Their flow equations are highly nonlinear and were solved via Runge-Kutta with shooting approach. It was finalized in the paper that adding the nanofluid rate of heat transport along with temperature distribution is much higher when compared to the microfluid. Koca *et al.,* [8] recently reviewed the size of the particle's impact on nanofluid viscosity. The latest work of Bowers *et al.,* [9] introduced the heat transport efforts of nanofluids motions in microchannels. It was noticed in their study that huge viscosity of nanofluids when compared with water, power pumping which is needed in the driving movement of nanofluid in microchannels enhancement.

There are numerous uses for bioconvection in biotechnology along with biological system. Kuznetsov [10] examined the initiation of natural convection flow in a heterogeneous mixture of gyrotactic/oxytactic microorganisms in various scenarios and conducted structural analysis. The term bioconvection was described by Nield and Bejan [11] as "pattern creation in suspensions of microorganisms, including such algae and bacteria due to up-swimming of the microorganisms." Gravitational, gyrotaxis, and oxytaxis organisms are examples of these microorganisms. Many researchers have examined various elements of bioconvection. Kuznetsov [12] have explored the significance of particles on bioconvection firmness. He also investigated the influence of tiny solid particles in a dilute mixture having gyrotactic bacteria. To regulate the influence of bioconvection on small solid particles, they developed the concept of effective diffusivity. Aziz *et al.,* [13] recently investigated the steady free convection progression over a horizontal flat plate in a penetrable region filled with a water-based nanofluid containing gyrotactic bacteria.

Many scholars have highlighted the study of MHD due to its industrial uses. Daba and Devaraj [14] presented mixed convective flow by examining impact of relevant flow parameters in an accelerated regime. Jha *et al.,* [15] investigated free convective unstable Couette flow. The research

found that the magnetic generates Lorentz force, which reduce the electrically conducting fluid's mechanism Chemically reacting hydromagnetic unsteadiness. Malik *et al.,* [16] used the conjugate gradient technique along with the sufficient descent criterion to produce a new variable. Abas and Yatim [17] investigated the going to travel-wave equivalence solution for a gravity-driven non-Newtonian fluid stream. Malik *et al.,* [18] investigated the convergence of a new coefficient conjugate gradient technique. A study of MHD progression of nanofluid in the context of viscous depletion was explained by Alsagri *et al.,* [19]. The study employed the Adomian decomposition approach and determined that fluid temperature improves when the Hartmann number increases. Teh and Ashgar [20] studied three-dimensional MHD hybrid nanofluid flow by considering Joule heating significance. Fekadu and Harish [21] elucidated numerical studies on thermo-hydraulic characteristics of turbulent flow in a tube on a twisted tape. Thermal radiation in nanofluid permeable flow bounded with partial slip condition was investigated by Rusdi *et al.,* [22]. Ebenezer *et al.,* [23] recently investigated incidence of manifold slip-on reaction and transport in magneto-bioconvective and magnetic nanoparticles power law flow between two parallel plates. In another study, Falodun and Ige [24] investigated magneto-thermal and chemical reactions on the Casson-Williamson nanofluids flow using regression analysis. Latib and Kamaruzaman [25] conducted simulation study on the heat performance of different nanofluids for rotating detonation engine cooling. MHD mixed convection of viscoelastic nanofluid flow due to constant heat flux was investigated by Mahat *et al.,* [26]. Sharafatmandjoor [27] studied effects of imposition of viscous and thermal forces on dynamical features of swimming of a microorganism in nanofluids. The identification of flow regime in Gas-liquid two-phase flow in horizontal pipe by deep learning was investigated by Khan *et al.,* [28]. Omar *et al.,* [29] explored analytical solution on performance of unsteady Casson fluid with thermal radiation and chemical reaction. Idowu and Falodun [30] studied variable thermal conductivity and viscosity effects on non-Newtonian fluids flow through a vertical porous plate.

Based on our investigation, no study (research) literature has considered the applications of Nanoparticles on bioconvection flow of non-Newtonian fluid alongside Gyrotactic microorganisms with thermal radiation, Soret-Dufour mechanisms and Joule heating. The analysis of Venkata *et al.,* [31] on impact of Soret and Dufour on MHD Casson fluid flow past a stretching surface with convective-diffusive conditions explored the flow of Casson fluid in the absence of gyrotactic microorganisms, and in the previous study Casson fluid was considered in the absence of Joule heating on the motion of Casson nanofluids within the boundary layer. The study of Venkata *et al.,* [31] has been extended in this research to fill the gap missed. In the previous study, Casson fluid was considered in the absence of Joule heating and Gyrotactic microorganisms but the present analysis shall consider the influence of Joule heating and viscous dissipation on the Casson nanofluid movement within the boundary layer where gyrotactic microorganisms are situated. Therefore, this study is set to consider the numerous applications of bioconvection flow of non-Newtonian fluid and nanotechnology in biomedical and environmental applications. The model equations in this work shall be solved in this research using the spectral relaxation approach (method). The spectral relaxation method uses the basic concept of the Gauss-Seidel techniques in decoupling and linearizing the nonlinear terms.

2. Mathematical Model

A two-dimensional, incompressible, laminar, bioconvective fluid movement with nanoparticles across a vertical plate are considered. T_w and C_w are the temperature and concentration-dependent volume fractions of nanoparticles. In addition, C_∞ denote free stream concentration while T_∞ stands for free stream. The Rosseland approximation applied to analyse the radiative heat flow of optically

thin nanofluids. The inclined plate's surface is assumed to be porous, allowing fluid wall injection or suction to pass through, with carefully considering of the effect of Joule heating, also to consider the viscous depletion, and Soret-Dufour techniques. The motion of the Casson nanofluids is move due to the stretchable of the slanting surface of the plate, and also in the y-axis direction, a uniform strength magnetic field (B_0) is applied. Figure 1 shows the physical interpretation of the fluid model. The model specie concentration is thought to be excessive that the Soret and Dufour scenarios are believed to be unavoidable. A $T_w < T_\infty$ and $C_w < C_\infty$ scenario with a cooled slanting plate is explored.

The scenario of Idowu and Falodun [30] as $\left(\tau = \mu \frac{\partial u}{\partial y}|_y = 0\right)$ in compliance with Fredrickson [32] described in the manner using the flow constitutive equations for Casson fluid as below

$$\tau_{ij} = \left(\mu_b(T) + \frac{P_y}{\sqrt{2\pi}}\right) 2e_{ij} \quad \text{when} \quad \pi > \pi_c$$
$$\tau_{ij} = \left(\mu_b(T) + \frac{P_y}{\sqrt{2\pi_c}}\right) 2e_{ij} \quad \text{when} \quad \pi < \pi_c \tag{1}$$

Where P_y represents the yield stress and is expressed in mathematical form

$$P_y = \frac{\mu_b(T)\sqrt{(2\pi)}}{\beta} \tag{2}$$

μ_b defines plastic viscosity, $\pi = e_{ij}$ denotes the constituent product of the distortion rate e_{ij} denotes the distortion rate, and π_c denotes the critical value based on Casson fluid and β is the casson fluid. The Casson fluid motion where $\pi > \pi_c$, is as follows

$$\mu_0 = \mu_b(T) + \frac{P_y}{\sqrt{2\pi}} \tag{3}$$

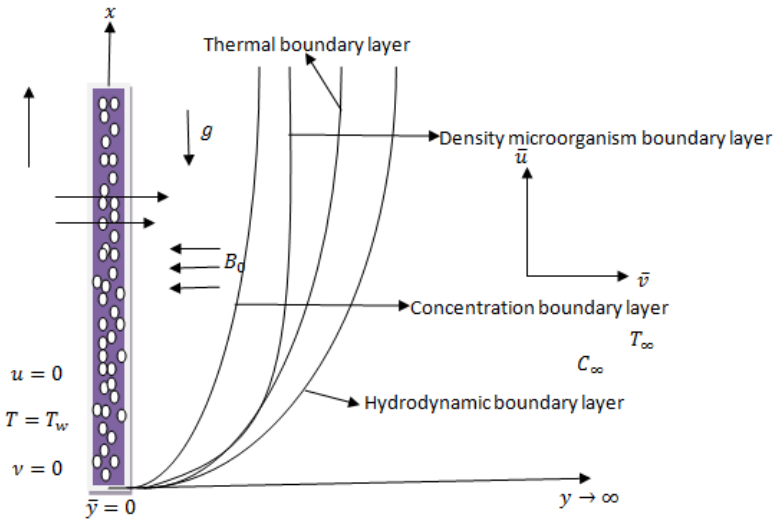

Fig. 1. The figure above (boundary layer) shows how the problem is physically configured

When Eq. (2) is substituted in Eq. (3), the kinematic viscosity becomes subject to μ_b which is the plastic dynamic viscosity, then also for density and Casson term which are ρ, and β respectively they yield to:

$$\mu_0 = \frac{\mu_b(T)}{\rho}\left(1+\frac{1}{\beta}\right) \tag{4}$$

The boundary layer approximation is investigated since it is believed that the Boussinesq approximation is accurate. Using the previously stated principles, the following equations are generated

$$\frac{\partial u}{\partial x}+\frac{\partial v}{\partial y}=0 \tag{5}$$

$$u\frac{\partial u}{\partial x}+v\frac{\partial u}{\partial y}=\nu\left(1+\frac{1}{\beta}\right)\frac{\partial^2 u}{\partial y^2}-\frac{\sigma B_0^2}{\rho}u+g\beta_t(T-T_\infty)+g\beta_c(C-C_\infty)-\frac{\nu}{K}u+g\beta_n(N-N_\infty) \tag{6}$$

$$\frac{\partial T}{\partial x}+v\frac{\partial T}{\partial y}=\alpha\frac{\partial^2 T}{\partial y^2}-\frac{1}{\rho c_p}\frac{\partial q_r}{\partial y}+\frac{\nu}{c_p}\left(1+\frac{1}{\beta}\right)\left(\frac{\partial u}{\partial y}\right)^2+\frac{\sigma B_0^2}{c_p\rho}u^2+\frac{Dk_T}{c_s c_p}\frac{\partial^2 C}{\partial y^2}+\tau\left[D_B\left(\frac{\partial C}{\partial y}\right)\left(\frac{\partial T}{\partial y}\right)+\frac{D_T}{T_\infty}\left(\frac{\partial T}{\partial y}\right)^2\right] \tag{7}$$

$$u\frac{\partial C}{\partial x}+v\frac{\partial C}{\partial y}=D_B\frac{\partial^2 C}{\partial y^2}+\frac{D_T}{T_\infty}\frac{\partial^2 T}{\partial y^2}-k_l(C-C_\infty)+\frac{Dk_T}{T_m}\frac{\partial^2 T}{\partial y^2} \tag{8}$$

$$u\frac{\partial N}{\partial x}+v\frac{\partial N}{\partial y}=D_n\frac{\partial^2 N}{\partial y^2}-\frac{bW_c}{\Delta C}\left(\frac{\partial N}{\partial y}\frac{\partial C}{\partial y}+\frac{\partial^2 C}{\partial y^2}\right) \tag{9}$$

Subject to the boundary constraints

$$\begin{gathered} u=Bx \quad ,v=-v(x) \quad ,T=T_w \quad ,C=C_w \text{ , at } \quad y=0 \\ u\longrightarrow 0 \quad ,T\longrightarrow T_\infty \quad ,C\longrightarrow C_\infty \quad \text{, as} \quad y\longrightarrow\infty \end{gathered} \tag{10}$$

u and v denotes the relations $u=\frac{\partial\psi}{\partial y}$ also $v=-\frac{\partial\psi}{\partial x}$. where it is defined of u and v, $\psi(x,y)$ is for automated free stream which satisfies the equation continuity. The definition of similarity variables is

$$\eta=\left(\frac{B}{\nu}\right)^{\frac{1}{2}}y \quad ,\psi=(\nu B)^{\frac{1}{2}}xf(\eta),\ \ \theta(\eta)=\frac{T-T_\infty}{T_w-T_\infty},\ \ \phi(\eta)=\frac{C-C_\infty}{C_w-C_\infty} \tag{11}$$

By using the similarity variables defined above on the flow Eq. (5) to Eq. (9) subject to Eq. (10) yields

$$\left(1+\frac{1}{\beta}\right)f'''+ff''-(f')^2-\left(M+\frac{1}{Po}\right)f'+Gt\theta+Gc\phi+Gm\varphi=0 \tag{12}$$

$$\left(\frac{1+R}{Pr}\right)\theta''+f\theta'+Ec(f'')^2+MEc(f')^2+Du\phi''+Nb\phi'\theta'+Nt(\theta')^2=0 \tag{13}$$

$$\phi'' + \frac{ScNt}{LnNb}\theta'' - ScCr\phi + ScSr\theta'' + Scf\phi' = 0 \tag{14}$$

$$\varphi'' + Lbf\varphi' - LbPe\left(\varphi'\phi' + \phi''(\varphi + \beta_k)\right) = 0 \tag{15}$$

Subject to

$$f' = 1,\ f = f_w,\ \theta = 1,\ \phi = 1, \quad at \quad \eta = 0 \tag{16}$$

$$f' \longrightarrow 0,\ \theta \longrightarrow 0,\ \phi \longrightarrow 0, \quad as \quad \eta \longrightarrow \infty \tag{17}$$

The pertinent parameters controlling the flow are defined as follows: M is Magnetic parameter, Po is Permeability parameter, Gt is Thermal Grashof number, Gc is Mass Grashof number, Gm is Motile density Grashof number, R is Thermal radiation parameter, Pr is Prandtl number, Ec is Eckert number, Du is Dufour parameter, Nb is Brownian motion parameter, Nt is Thermophoresis parameter, Ln is Lewis number, Sc is Schmidt number, Lb is Lewis number, Pe is Peclet number, β_k is Constant, Cr is chemical reaction parameter, Sr is Soret number. The technical amounts of examination (engineering quantities) are (Nu_x) the local Nusselt, local Sherwood number (Sh_x), local motile density number (Nn_x) and skin friction coefficient (Cf) as follows

$$Cf = \frac{\tau_w}{\rho(U_w)^2}, \qquad Nu_x = \frac{q_w}{K(T_w - T_\infty)}, \qquad Sh_x = \frac{S_w}{D(C_w - C_\infty)}, \qquad Nn_x = \frac{q_m}{D_n(N_w - N_\infty)}$$

where

$$\tau_w = \left[\mu\left(1 + \frac{1}{\beta}\right)(u_y)|_{y=0}\right], \qquad q_w = -K(T_y)|_{y=0} - 4\sigma_0(3Ke)^{-1}(T_y^4)|_{y=0},$$

$$S_w = D(C_y)|_{y=0}, \qquad q_m = D_n(N_y)|_{y=0}$$

3. Spectral Relaxation Approach (SRM)

The proposed method of solutions is Spectral Relaxation Method. SRM employs the procedure of Gauss-Seidel techniques of relaxation to decouple and linearize the transformed coupled differential equations simultaneously. This method employed the Chebyshev pseudo-spectral approach to discretize the linearized set of equations. The linear tern is considered at the current iteration to be $r + 1$ while the nonlinear terms are considered at the previous iteration denoted by r.

The basic steps of the spectral approach are

i. Firstly, use Gauss-Siedel methods to decouple and linearize the nonlinear equations;
ii. Further discretization of the linearized equations; and
iii. Chebyshev pseudo-spectral approach is used to iteratively solve the discretized equations.

Employing the SRM on the non-linear Eq. (12) to Eq. (17) to yields

$$\left(1 + \frac{1}{\beta}\right)f'''_{r+1} + f''_{r+1}f_{r+1} - (f'_r)^2 - \left(M + \frac{1}{Po}\right)f'_{r+1} + Gt\theta_r + Gc\phi_r + Gm\varphi_r = 0 \tag{18}$$

$$\left(\frac{1+R}{Pr}\right)\theta''_{r+1} + f_{r+1}\theta'_{r+1} + Ec(f''_{r+1})^2 + MEc(f'_{r+1})^2 + Du\phi''_r + Nb\phi'_r\theta'_{r+1} + Nt(\theta'_{r+1})^2 = 0 \quad (19)$$

$$\phi''_{r+1} + \frac{ScNt}{LnNb}\theta''_{r+1} - ScCr\phi_{r+1} + ScSr\theta''_{r+1} + Scf_{r+1}\phi'_{r+1} = 0 \quad (20)$$

$$\varphi''_{r+1} + Lbf_{r+1}\varphi'_{r+1} - Pe\varphi'_{r+1}\phi'_{r+1} - Pe\phi''_{r+1}\varphi_{r+1} - Pe\beta_k\phi''_{r+1} = 0 \quad (21)$$

subject to

$$f_{r+1}(0,\eta) = f_w, \quad f'_{r+1}(0,\eta) = 1, \theta_{r+1}(0,\eta) = 1, \quad \phi_{r+1}(0,\eta) =, \ \varphi_{r+1}(0,\eta) = 1 \quad (22)$$

$$f'_{r+1}(\infty,\eta) \longrightarrow 0, \quad \theta_{r+1}(\infty,\eta) \longrightarrow 0, \quad \phi_{r+1}(\infty,\eta) \longrightarrow 0, \ \varphi_{r+1}(\infty,\eta) \longrightarrow 0 \quad (23)$$

setting

$$a_{0,r} = \left(1 + \frac{1}{\beta}\right), \qquad a_{1,r} = f_{r+1}, \qquad a_{2,r} = -f_{r+1}^2, \qquad a_{3,r} = -\left(M + \frac{1}{Po}\right),$$

$$a_{4,r} = Gt\theta_r + Gc\phi_r + Gm\varphi_r, \qquad b_{0,r} = \left(\frac{1+R}{Pr}\right), \qquad b_{1,r} = f_{r+1}, \qquad b_{2,r} = Ec(f''_{r+1})^2,$$

$$b_{3,r} = MEc(f'_{r+1})^2 + Du\phi''_r, \qquad b_{4,r} = Nb\phi'_r, \qquad b_{5,r} = Nt(\theta'_{r+1})^2, \qquad c_{0,r} = \frac{ScNt}{LnNb}\theta''_{r+1}$$

$$c_{1,r} = ScSr\theta''_{r+1}, \qquad c_{2,r} = Scf_{r+1}, \qquad d_{0,r}Lbf_{r+1}, \qquad d_{1,r} = -Pe\phi'_{r+1},$$

$$d_{2,r} = -Pe\phi''_{r+1}, \qquad d_{3,r} = -Pe\beta_k\phi''_{r+1}$$

Invoking the defined coefficient terms resulted to

$$a_{0,r}f'''_{r+1} + a_{1,r}f''_{r+1} + a_{2.r} + a_{3,r}f'_{r+1} + a_{1,r} = 0 \quad (24)$$

$$b_{0,r}\theta''_{r+1} + b_{1,r}\theta'_{r+1} + b_{2,r} + b_{3,r} + b_{4,r}\theta'_{r+1} + b_{5,r} = 0 \quad (25)$$

$$\phi''_{r+1} + c_{0,r} - ScCr\phi_{r+1} + c_{1,r} + c_{2,r}\phi'_{r+1} = 0 \quad (26)$$

$$\varphi''_{r+1} + d_{0,r}\varphi'_{r+1} + d_{1,r}\varphi'_{r+1} + d_{2,r}\varphi_{r+1} + d_{3,r} = 0 \quad (27)$$

subject to

$$f_{r+1}(0,\eta) = f_w, \quad f'_{r+1}(0,\eta) = 1, \ \theta_{r+1}(0,\eta) = 1, \quad \phi_{r+1}(0,\eta) = \varphi_{r+1}(0,\eta) = 1, \quad (28)$$

$$f'_{r+1}(\infty,\eta) \longrightarrow 0, \quad \theta_{r+1}(\infty,\eta) \longrightarrow 0, \quad \phi_{r+1}(\infty,\eta) \longrightarrow 0, \varphi_{r+1}(\infty,\eta) \longrightarrow 0 \quad (29)$$

The Gauss-Lobatto collocation is employed to name the undisclosed functions which is defined as

$$\xi_j = \cos\frac{\pi j}{N}, \quad j = 0,1,2,\ldots,N; \quad 1 \le \xi \le -1 \quad (30)$$

And $N =$ numeric collocation points. Solving all linearized equations, the main domain of the physical problem is taken $(0, \infty)$ to $(-1,1)$. The transformation used in mapping the problem interval together is defined as

$$\frac{\eta}{L} = \frac{\xi+1}{2}, \quad -1 \leq \xi \leq 1 \tag{31}$$

In the above, L is a scaling term which is employed to execute the constraints at infinity. The approximation for solving the Eq. (24) to Eq. (27) are acquired at $\eta = 0$ which was stated to confirm with the boundary constraints (28) and (29). Therefore $f_0(0,\eta), \theta_0(0,\eta), \varphi_0(0,\eta)$ and $\phi_0(0,\eta)$ are defined as

$$f_0(0,\eta) = f_w - e^{-\eta}, \quad \theta_0(0,\eta) = \phi_0(0,\eta) = \varphi_0(0,\eta) = e^{-\eta} \tag{32}$$

The Eq. (24) to Eq. (27) are tackled repeatedly for all undisclosed functions by from initial guess in Eq. (31). The schemes in Eq. (24), Eq. (25), Eq. (26) and Eq. (27) are tackled iteratively for $\varphi_{r+1}(0,\eta), f_{r+1}(0,\eta), \phi_{r+1}(0,\eta)$ and $\theta_{0,\eta}$ as $r = 0,1,2$. To get solution to Eq. (24) to Eq. (27), the Eq. (24) to Eq. (27) are discretized using Chebyshev spectral collocation technique in η-direction alongside implicit finite difference. The techniques of finite difference are now taken on together with centering about an average unknown function. Thus, utilizing the centering in functions $\phi(0,\eta), \theta(0,\eta)$ and $f(0,\eta)$ alongside their derivative leads to

$$\left(\frac{df}{d\eta}\right)^{n+\frac{1}{2}} = \frac{f_j^{n+1}-f_j^n}{\Delta\eta}, \quad \left(\frac{d\theta}{d\eta}\right)^{n+\frac{1}{2}} = \frac{\theta_j^{n+1}-\theta_j^n}{\Delta\eta}, \left(\frac{d\phi}{d\eta}\right)^{n+\frac{1}{2}} = \frac{\phi_j^{n+1}-\phi_j^n}{\Delta\eta}, \left(\frac{d\varphi}{d\eta}\right)^{n+\frac{1}{2}} = \frac{\varphi_j^{n+1}-\varphi_j^n}{\Delta\eta} \tag{33}$$

The notion of spectral collocation approach is the utilization of matrix differentiation D defined as

$$\frac{d^r f}{d\eta^r} = \sum_{k=0}^{N} D_{ik}^r u(\xi_k) = D^r f, \; \frac{d^r \theta}{d\eta^r} = \sum_{k=0}^{N} D_{ik}^r \theta(\xi_k) = D^r \theta, \quad i = 0,1,\dots N \tag{34}$$

$$\frac{d^r \phi}{d\eta^r} = \sum_{k=0}^{N} D_{ik}^r \phi(\xi_k) = D^r \phi, \frac{d^r \varphi}{d\eta^r} = \sum_{k=0}^{N} D_{ik}^r \varphi(\xi_k) = D^r \varphi, \quad i = 0,1,\dots N \tag{35}$$

Using the Chebyshev spectral method on Eq. (25) to Eq. (28) gives

$$a_{0,r} D^3 f_{r+1} + a_{1,r} D^2 f_{r+1} + a_{3,r} D f_{r+1} + a_{2,r} + a_{4,r} = 0 \tag{36}$$

$$b_{0,r} D^2 \theta_{r+1} + b_{1,r} D\theta_{r+1} + b_{4,r} D\theta_{r+1} + b_{2,r} + b_{3,r} + b_{5,r} = 0 \tag{37}$$

$$D^2 \phi_{r+1} + c_{2,r} D\phi_{r+1} - ScKr\phi_{r+1} + c_{0,r} + c_{1,r} = 0 \tag{38}$$

$$D^2 \varphi_{r+1} + d_{0,r} D\varphi_{r+1} + d_{1,r} D\varphi_{r+1} + d_{2,r} \varphi_{r+1} + d_{3,r} = 0 \tag{39}$$

subject to

$$f_{r+1}(0,\eta) = f_w, \quad f'_{r+1}(0,\eta) = 1, \theta_{r+1}(0,\eta) = 1, \quad \phi_{r+1}(0,\eta) = \varphi_{r+1}(0,\eta) = 1, \tag{40}$$

$$f'_{r+1}(\infty,\eta) \longrightarrow 0, \quad \theta_{r+1}(\infty,\eta) \longrightarrow 0, \quad \phi_{r+1}(\infty,\eta) \longrightarrow 0, \varphi_{r+1}(\infty,\eta) \longrightarrow 0 \tag{41}$$

4. Results and Discussions

The SRM has been utilized to resolve the transformed Eq. (12) to Eq. (15) alongside the boundary conditions in Eq. (16) and Eq. (17). The significant impact of all controlling parameters on motile density microorganisms $\varphi(\eta)$, temperature $\theta(\eta)$, concentration $\phi(\eta)$ and velocity $\left(1+\frac{1}{\beta}\right)f'(\eta)$ are represented with graphs. A numerical computation on skin friction, motile density, Nusselt along with Sherwood numbers for numerous parameters are furnish. Table 1 shows the computational values for flow parameters. A higher value of magnetic field parameter was observed to enhance the skin friction and has no impact on the Nux, Shx and Nnx respectively. A higher value of β in Table 1 influences the skin friction and the Nusselt number. An enhancement in skin friction and Nusselt number was observed for higher value of R, Pr and Ec.

Table 1
Computational values of pertinent flow parameters on the engineering quantities of interest

M	β	Po	Gt	Gc	Gm	R	Pr	Ec	Nb	Nt	Pe	Cf	Nu_x	Sh_x	Nn_x
0.5												0.3052	1.4851	1.5399	0.6881
1.0												1.4370	1.4851	1.5399	0.6881
1.5												1.9333	1.4851	1.5399	0.6881
	1.0											0.5651	0.2085	2.0012	0.7171
	2.0											1.0714	1.5959	2.0012	0.7171
	3.0											1.5778	1.9833	2.0012	0.7171
		2.0										0.3119	1.4851	2.5191	0.6470
		3.0										0.6675	1.6069	2.8402	0.6470
		4.0										1.0349	1.7323	3.1502	0.6470
			0.0									0.9811	0.5365	0.8113	0.4388
			0.5									1.2351	0.5365	0.8113	0.4388
			1.0									2.1583	0.5365	0.8113	0.4388
				0.0								1.5361	0.5635	0.8633	0.5179
				0.5								2.7403	0.5635	0.8633	0.5179
				1.0								3.9445	0.5635	0.8633	0.5179
					0.0							1.5944	0.5647	0.9421	0.8678
					0.5							2.3373	0.5799	0.9421	0.9245
					1.0							2.7553	0.5884	0.9421	0.9560
						0.5						1.7592	0.5304	0.7968	0.6141
						1.0						1.9239	0.5481	0.7968	0.6141
						1.5						2.0278	0.6184	0.7968	0.6141
							0.71					1.5316	0.5651	0.8112	0.0240
							3.0					1.1421	0.9259	0.8112	0.0240
							7.0					0.9902	1.4851	0.8112	0.0240
								0.3				1.5076	0.1952	0.9910	0.5911
								0.5				1.7323	0.3106	0.9910	0.5911
								0.7				2.1249	0.6002	0.9910	0.5911
									2.0			1.7058	0.2501	0.8611	0.4120
									4.0			2.2534	0.3709	0.8611	0.4120
									6.0			3.2098	1.3351	0.8611	0.4120
										2.0		1.7176	0.4911	0.1205	0.5001
										4.0		2.3033	0.4911	0.6305	0.5001
										6.0		3.3264	0.4911	1.4323	0.5001
											0.2	0.4109	1.4861	0.3926	0.6391
											0.5	1.8061	1.9931	0.3926	0.7991
											0.8	2.6268	2.2670	0.3926	0.8400

Table 2 shows an increase in Sc and Cr degenerates the skin friction but increases the Sherwood number. Table 3 shows the correctness of the present study and that of Venkata *et al.,* [31].

Table 2
Computational values of skin friction, Nusselt and Sherwood numbers for pertinent flow parameters

Sc	Cr	Lb	Cf	Nu_x	Sh_x	Nn_x
0.31			2.2071	0.4056	0.5847	0.9221
0.61			1.9565	0.4056	0.6125	0.9221
1.0			1.8016	0.4056	0.6671	0.9221
	0.3		0.5825	0.8550	0.8023	0.6912
	0.6		1.5060	0.8550	0.9023	0.6912
	0.9		1.3970	0.8550	1.0406	0.6912
		0.01	0.3219	1.4291	1.8999	1.5191
		0.06	1.0349	1.7223	1.8999	2.1402
		0.1	1.4144	1.8610	1.8999	3.4498

Table 3
Comparison of the present study with that of Venkata *et al.,* [31]

			Venkata *et al.,* [31]			Present outcomes		
Sr	Du	Sc	Cf	Nu	Sh	Cf	Nu	Sh
0.1			-1.0819	0.4790	0.5947	-1.0820	0.4791	0.5948
0.3			-1.0790	0.4866	0.5813	-1.0791	0.4867	0.5814
0.5			-1.0760	0.4944	0.5670	-1.0761	0.4945	0.5671
	0.1		-1.0805	0.4832	0.5882	-1.0804	0.4831	0.5881
	0.3		1.0808	0.4556	0.5900	1.0807	0.4555	0.5901
	0.5		-1.0810	0.4268	0.5919	-1.0809	0.4267	0.5920
		0.5	-1.0755	0.4868	0.5461	-1.0753	0.4866	0.5459
		1.0	-1.0947	0.4717	0.7179	-1.0945	0.4715	0.7177
		1.5	-1.1057	0.4637	0.8336	-1.1055	0.4635	0.8334

Figure 2 shows the significance of Casson parameter on velocity contour, a notable enhancement in velocity contour due to growth in Casson term. A blood based Casson fluid is considered in this paper. A steady flow of the blood Casson fluid is observed in the vessels when $\beta = 0.2,\ 0.4$ and 0.6. A more increase in β (that is, $\beta \longrightarrow \infty$) the refused to flow and the present model changed to Newtonian fluid at $\beta \longrightarrow \infty$. Physically, an increase in β means that the yield exhibiting fluid increases inside the boundary layer. Hence, the plastic viscosity alongside the depth of hydrodynamic boundary layer increases.

Figure 3 displays the significance of magnetic parameter on velocity contour, a diminish in the velocity contour was observed by decrease in $\mathrm{M} = 1,2$, and 3. The perpendicular imposition of magnetic parameter to the progression leads to Lorentz force. Generally, the Lorentz force creates resistance to the flow of an electrically conducting fluids.

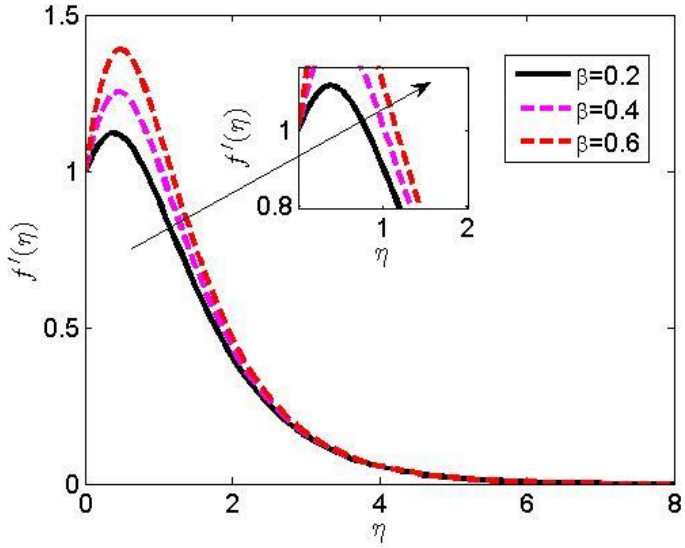

Fig. 2. Significance of Casson parameter on velocity contour

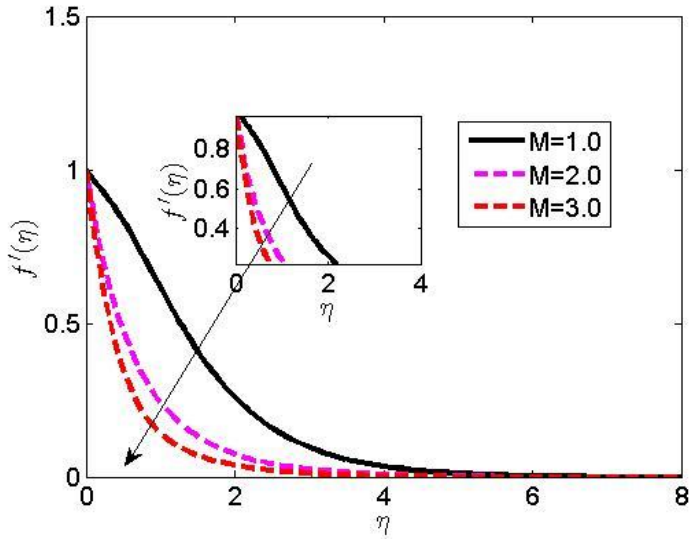

Fig. 3. Significance of magnetic parameter on velocity contour

Figure 4 shows the consequence of permeability parameter on velocity along with temperature contour, a considerable growth in the velocity along with temperature contour is noticeable with growth of Po. As $\mathrm{Po} = 0.1, 0.2,$ and 0.3 the holes allow more passage of blood flow within the layers. also, the temperature increases due to collision of blood particles within the layers. Hence, the thickness of thermal and hydrodynamic boundary layer increases within the boundary layer as the value of Po increases.

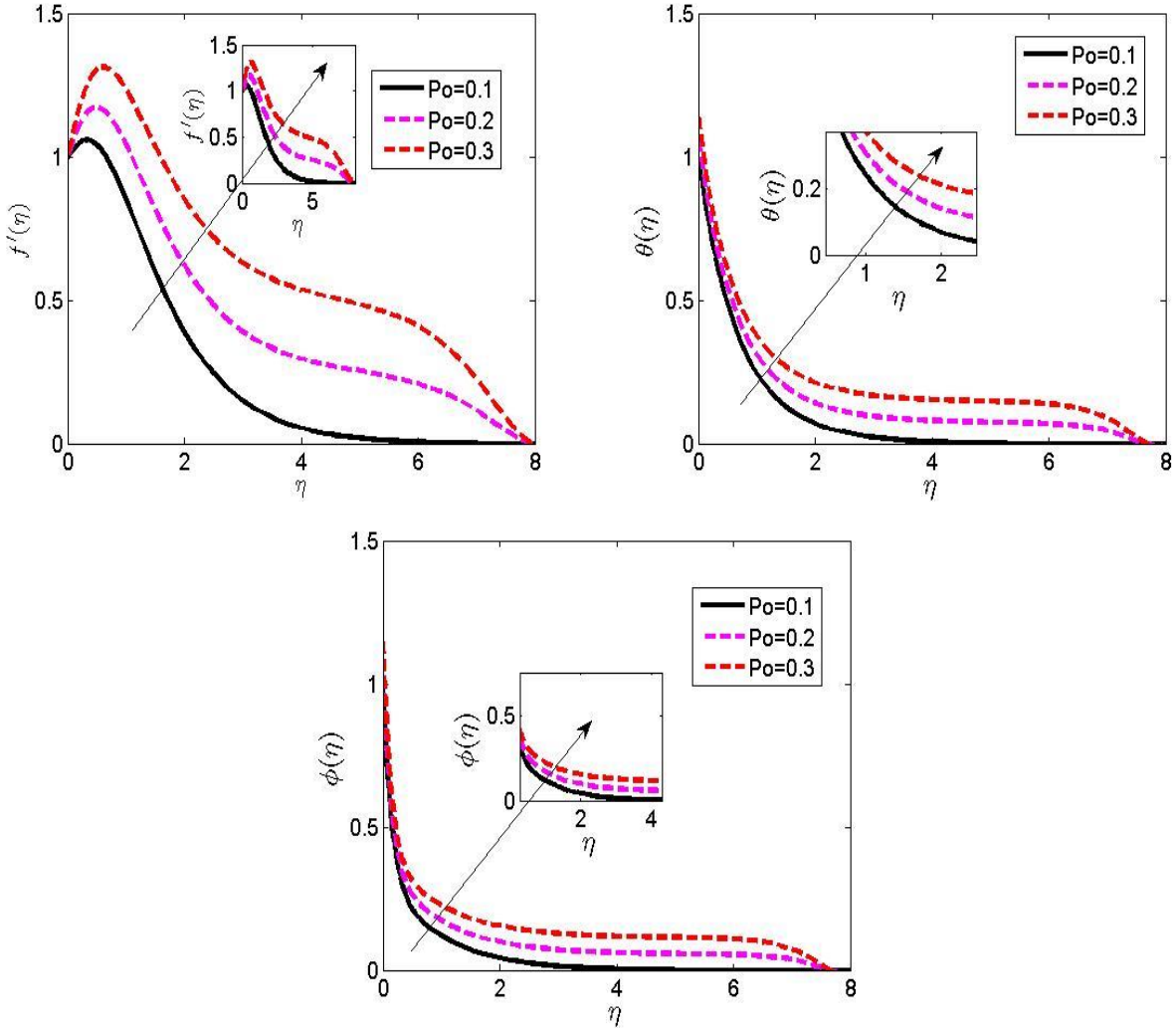

Fig. 4. Consequence of permeability parameter on velocity along with temperature contour

Figure 5 expose the significance of thermal, mass and motile density Grahsof numbers on velocity contour and enhancement in the velocity contour is noticeable as the values of $\mathrm{Gt} = \mathrm{Gc} = \mathrm{Gm} = 0.0, 0.5 \text{ and } 1.0$ increases. The Gt, Gc and Gm are buoyancy forces which acts on the fluid. This buoyancy forces helps to boost the fluid velocity and the entire boundary layer thickness.

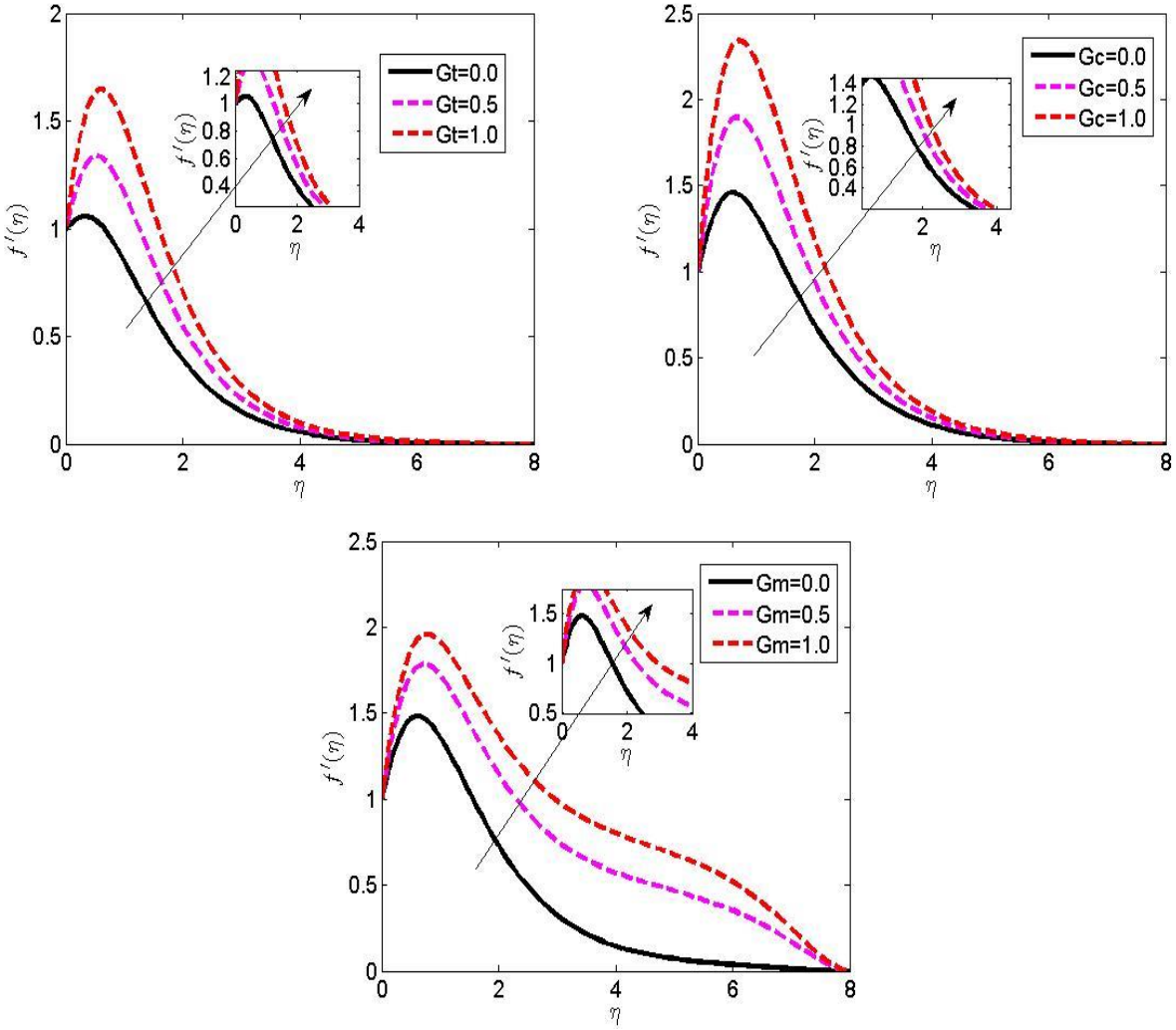

Fig. 5. Significance of thermal, mass and motile density Grahsof numbers on velocity contour

Figure 6 exhibit the significance of thermal radiation parameter on velocity along with temperature contours, a considerable increase in R shows increase in the velocity along with temperature profiles. A growth in R leads to increase in both thermal and hydrodynamic boundary layer thickness. Physically it means thermal energy greatly altered the flow regime within the boundary layer.

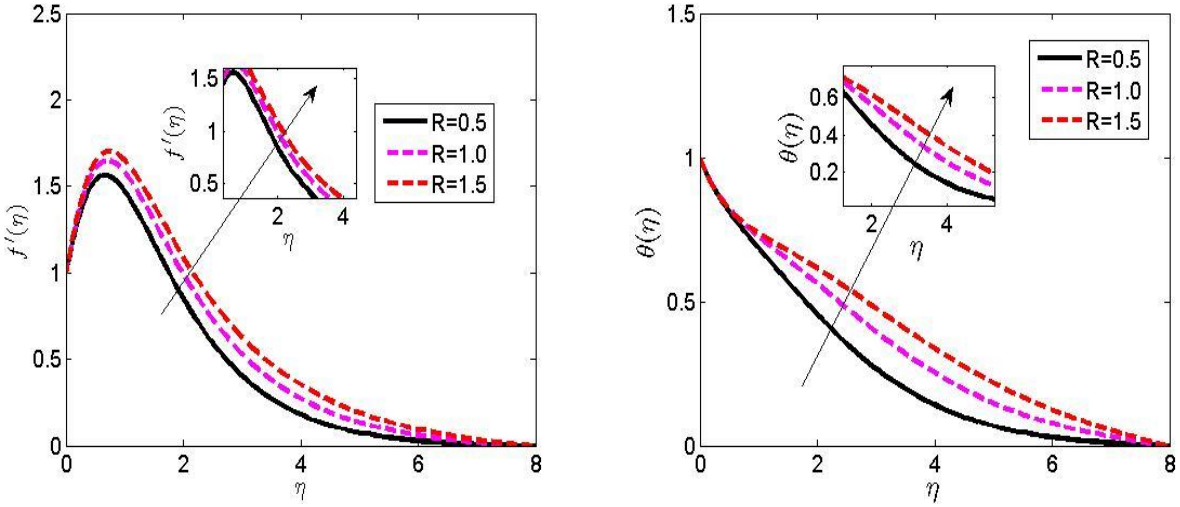

Fig. 6. Significance of thermal radiation parameter on velocity along with temperature contours

Figure 7 shows the significance of Prandtl number on velocity along with temperature contours. The Prandtl number (Pr) explains the mutual relationship between the thermal conductivity and kinematic viscosity. A growth in Pr leads to drastically lessens in velocity along with temperature profiles. This means that the heat diffuses greatly at higher Pr.

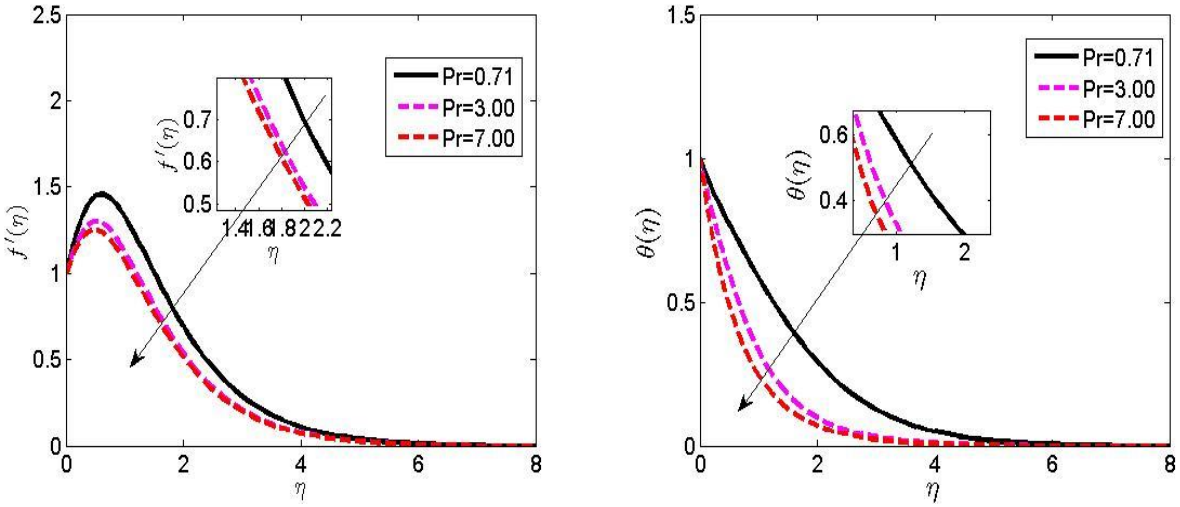

Fig. 7. Significance of Prandtl number on velocity along with temperature contours

Figure 8 display the significance of Eckert number on velocity along with temperature contours. An increase in Ec is observed to enhance the velocity along with temperature profiles. The Eckert is gotten from the viscous depletion term added to the energy equation. A growth in Ec raises the heat energy which enlarges the thickness of thermal boundary layer.

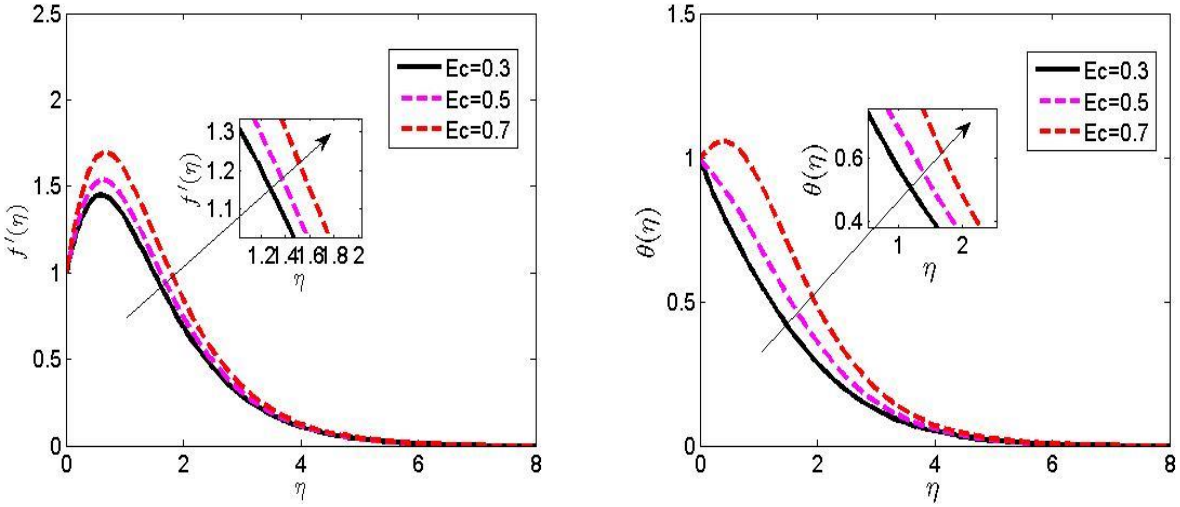

Fig. 8. Significance of Eckert number on velocity along with temperature contours

Figure 9 shows the significance of Brownian motion parameter on velocity along with temperature contours, a growth in Nb is noticed to enhance the velocity along with temperature contours. Practically, a considerable increase in Nb enhances the thickness of the hydrodynamic and thermal boundary layer.

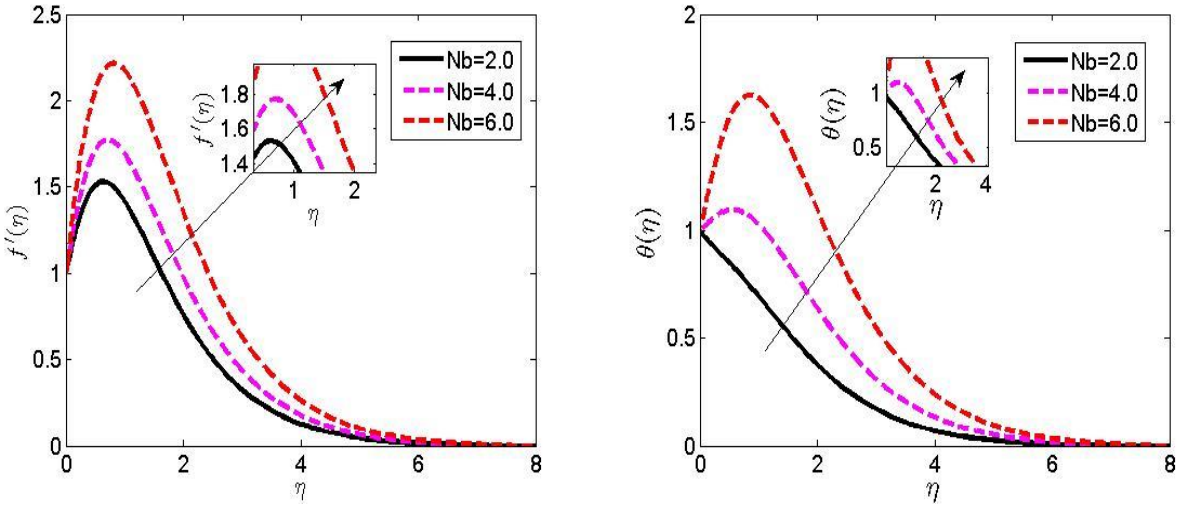

Fig. 9. Significance of Brownian motion parameter on velocity along with temperature contours

Figure 10 shows the significance of thermophoresis parameter on velocity along with concentration contours. A growth in Nt is noticed to enhance the velocity along with concentration contours. Thermophoresis defines the igration of particles from cold region to hot region. It describes the mixture of particles exhibiting distinct responses to temperature gradients. Therefore, increase in Nt enhances the hydrodynamic and concentration boundary layer thickness.

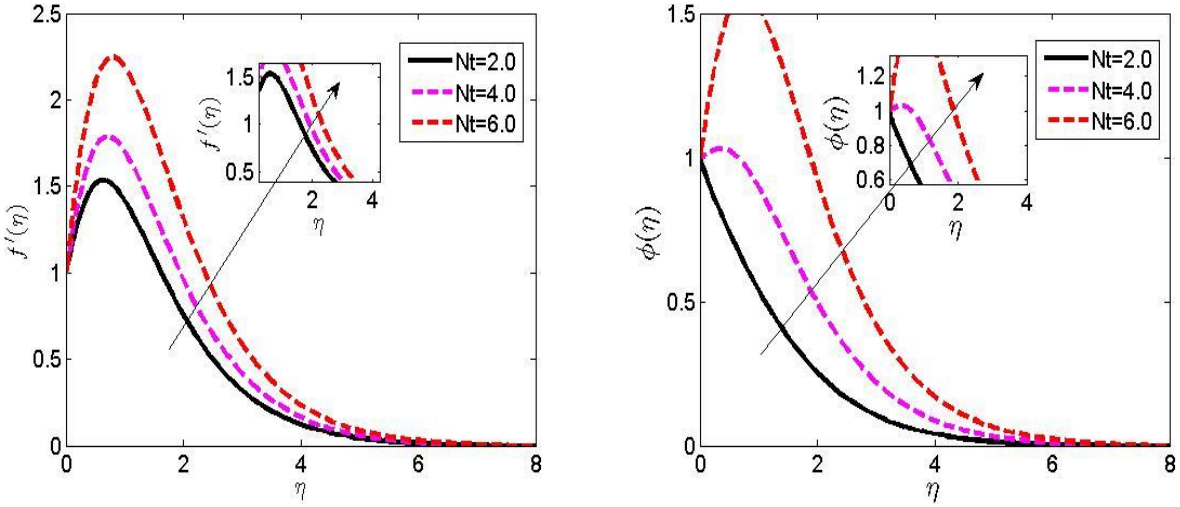

Fig. 10. Significance of thermophoresis parameter on velocity along with concentration contours

Figure 11 exhibit the significance of Peclet number on velocity along with motile density contours. A growth in Pe shows higher in the velocity and motile density profiles. Hence, an enhancement in the thickness of motile density boundary layer is noticeable. This aids the distribution of the motile microorganisms within the boundary layer.

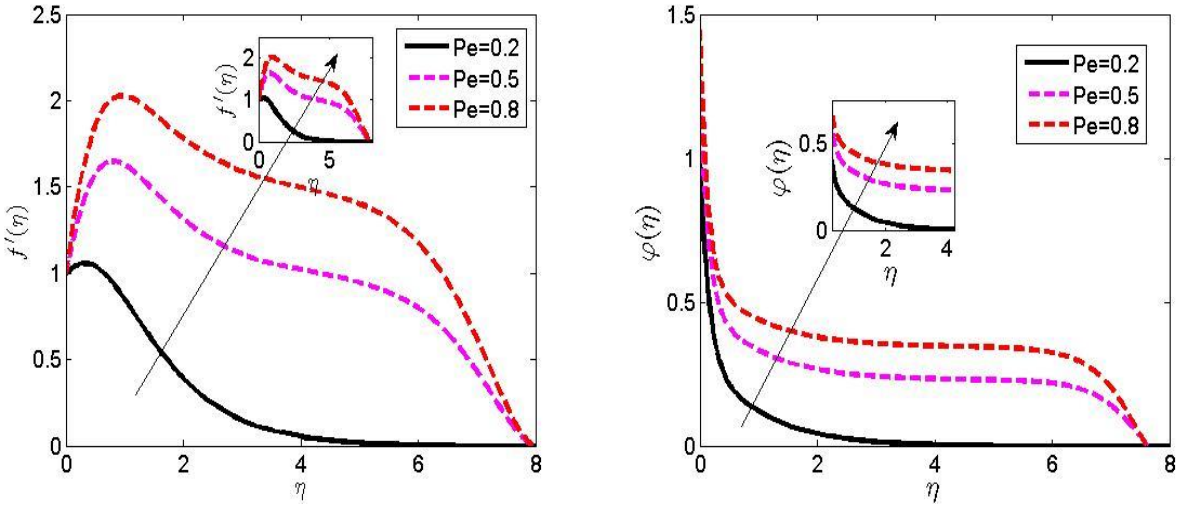

Fig. 11. Significance of Peclet number on velocity along with motile density contours

Figure 12 shows the significance of Schmidt number on velocity along with concentration contours. The Schmidt number describes the ratio of kinematic viscosity and mass diffusivity of fluid. Physically, when kinematic viscosity is greater than mass diffusivity, an increase in concentration profile is noticed for variable viscosity. Hence, a decrease in velocity and concentration profiles is observed for a constant viscosity considered in this paper. Physically, an increase in Sc shows a decrease in the thickness of hydrodynamic and concentration boundary layer.

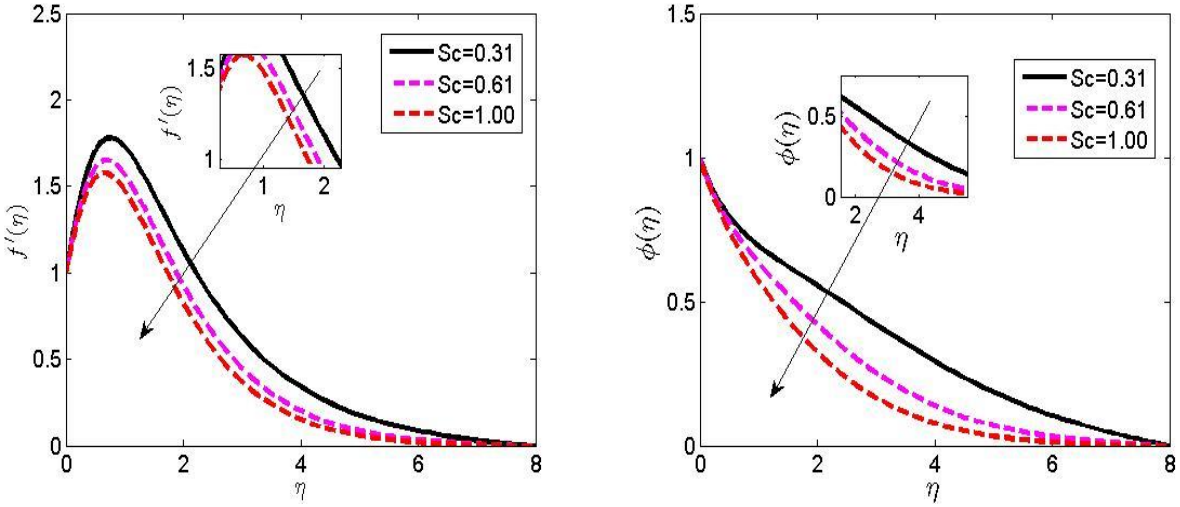

Fig. 12. Significance of Schmidt number on velocity along with concentration contours

Figure 13 shows significance of chemical reaction parameter on velocity along with concentration contours. A growth in Cr is noticed to lessen the velocity along with concentration contours. Hence, the thickness of the hydrodynamic boundary layer decreases.

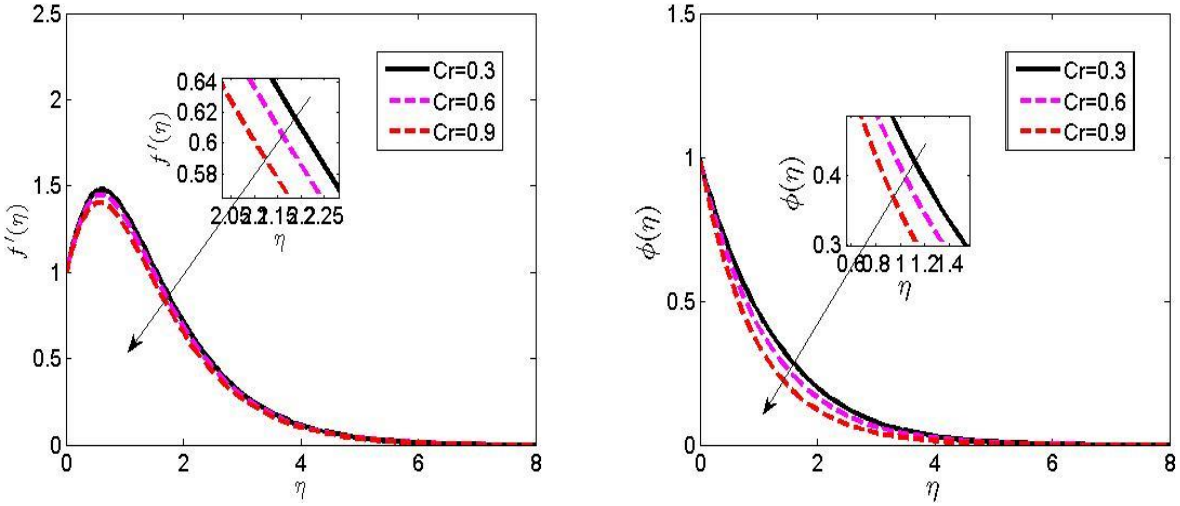

Fig. 13. Significance of chemical reaction parameter on velocity along with concentration contours

Figure 14 shows the significance of Lewis number on velocity along with motile density contours. A growth in Lb increase the velocity and motile density contours.

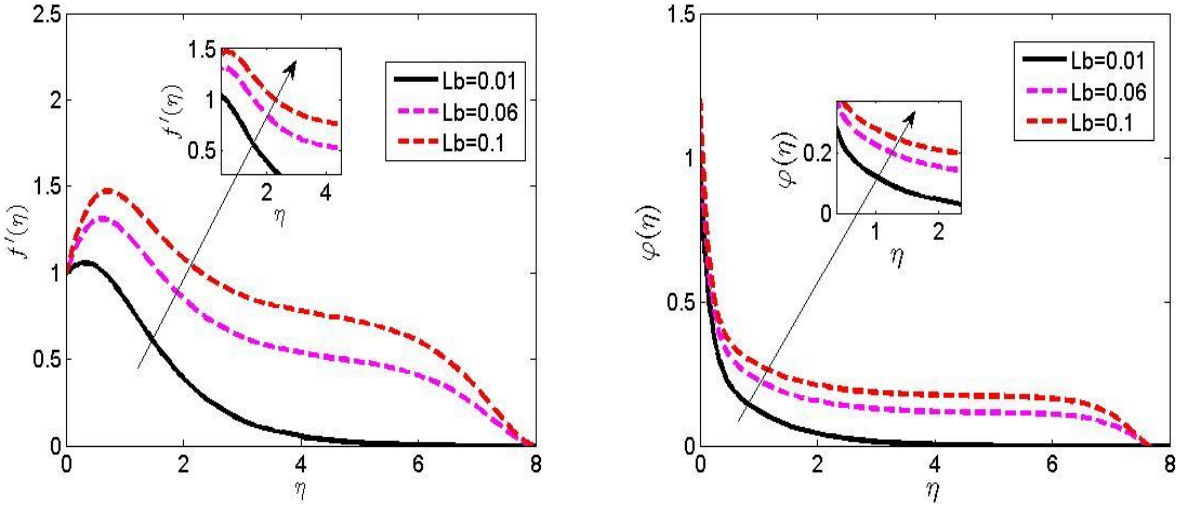

Fig. 14. Significance of Lewis number on velocity along with motile density contours

5. Conclusion

This study elucidated the analysis of free convective Casson fluid flow past a permeable vertical plate with gyrotactic microorganisms. This study was examined in the presence of pertinent flow parameters such as buoyancy force parameters, thermal radiation, chemical reaction parameter, Soret-Dufour mechanisms and so on. The present analysis considered a constant viscosity and thermal conductivity. The physics of the problem on physical parameters are shown using graphical results. The outcomes of the study are gotten by solving the coupled nonlinear ordinary differential Eq. (12) to Eq. (15) alongside the boundary constraints in Eq. (16) and Eq. (17). The key findings in this study are

i. The imposed magnetic field parameter was found to produce Lorentz force which slows down the motion of an electrically conducting fluid such as Casson fluid;
ii. The Casson parameter (β) was found to enhance the velocity and the hydrodynamic boundary layer;
iii. The existence of thermal radiation was found to raise the fluid temperature and thickness of thermal boundary layer;
iv. A considerable growth in the Eckert was noticed to enhance the fluid velocity and temperature by producing heat energy and
v. A decrease in skin friction and Nusselt number was noticed due to increase in Prandtl number.

Acknowledgments

The authors would like to express their gratitude to Universiti Sultan Zainal Abidin, Malaysia, whose comments and suggestions improved the work, as well as Tertiary Education Trust Fund (TETFund), Nigeria, for providing financial support for the MSc. via an Academic Staff Training Fellowship.

References

[1] Maschhoff, Paul, Sebastian Heene, Antonina Lavrentieva, Thorleif Hentrop, Christian Leibold, Marc-Nils Wahalla, Nils Stanislawski, Holger Blume, Thomas Scheper, and Cornelia Blume. "An intelligent bioreactor system for the cultivation of a bioartificial vascular graft." *Engineering in Life Sciences* 17, no. 5 (2017): 567-578. https://doi.org/10.1002/elsc.201600138

[2] Ahmed, Lukman O., Bidemi O. Falodun, and Jimoh Abdulwaheed. "Mechanism of Soret-Dufour, magnetohydrodynamics, heat and mass transfer flow with buoyancy force, and viscous dissipation effects." *Heat Transfer* 49, no. 5 (2020): 2831-2848. https://doi.org/10.1002/htj.21748
[3] Bahiraei, Mehdi. "Impact of thermophoresis on nanoparticle distribution in nanofluids." *Results in Physics* 7 (2017): 136-138. https://doi.org/10.1016/j.rinp.2016.12.012
[4] Seferis, I. E., J. Zeler, C. Michail, S. David, I. Valais, G. Fountos, N. Kalyvas et al. "Grains size and shape dependence of luminescence efficiency of Lu2O3: Eu thin screens." *Results in physics* 7 (2017): 980-981. https://doi.org/10.1016/j.rinp.2017.02.015
[5] Abdollahi, Ayoub, H. A. Mohammed, Sh M. Vanaki, A. Osia, and MR Golbahar Haghighi. "Fluid flow and heat transfer of nanofluids in microchannel heat sink with V-type inlet/outlet arrangement." *Alexandria Engineering Journal* 56, no. 1 (2017): 161-170. https://doi.org/10.1016/j.aej.2016.09.019
[6] Ahmed, Sameh E., and Z. Z. Rashed. "MHD natural convection in a heat generating porous medium-filled wavy enclosures using Buongiorno's nanofluid model." *Case Studies in Thermal Engineering* 14 (2019): 100430. https://doi.org/10.1016/j.csite.2019.100430
[7] Upadhya, S. Mamatha, C. S. K. Raju, and S. Saleem. "Nonlinear unsteady convection on micro and nanofluids with Cattaneo-Christov heat flux." *Results in Physics* 9 (2018): 779-786. https://doi.org/10.1016/j.rinp.2018.03.036
[8] Koca, Halil Dogacan, Serkan Doganay, Alpaslan Turgut, Ismail Hakki Tavman, R. Saidur, and Islam Mohammed Mahbubul. "Effect of particle size on the viscosity of nanofluids: A review." *Renewable and Sustainable Energy Reviews* 82 (2018): 1664-1674. https://doi.org/10.1016/j.rser.2017.07.016
[9] Bowers, James, Hui Cao, Geng Qiao, Qi Li, Gan Zhang, Ernesto Mura, and Yulong Ding. "Flow and heat transfer behaviour of nanofluids in microchannels." *Progress in Natural Science: Materials International* 28, no. 2 (2018): 225-234. https://doi.org/10.1016/j.pnsc.2018.03.005
[10] Kuznetsov, A. V. "The onset of thermo-bioconvection in a shallow fluid saturated porous layer heated from below in a suspension of oxytactic microorganisms." *European Journal of Mechanics-B/Fluids* 25, no. 2 (2006): 223-233. https://doi.org/10.1016/j.euromechflu.2005.06.003
[11] Nield, Donald A., and Adrian Bejan. *Convection in porous media*. Vol. 3. New York: springer, 2006.
[12] Kuznetsov, A. V. "The onset of nanofluid bioconvection in a suspension containing both nanoparticles and gyrotactic microorganisms." *International Communications in Heat and Mass Transfer* 37, no. 10 (2010): 1421-1425. https://doi.org/10.1016/j.icheatmasstransfer.2010.08.015
[13] Aziz, A., W. A. Khan, and I. Pop. "Free convection boundary layer flow past a horizontal flat plate embedded in porous medium filled by nanofluid containing gyrotactic microorganisms." *International Journal of Thermal Sciences* 56 (2012): 48-57. https://doi.org/10.1016/j.ijthermalsci.2012.01.011
[14] Daba, Mitiku, and Ponnaian Devaraj. "Unsteady hydromagnetic chemically reacting mixed convection flow over a permeable stretching surface with slip and thermal radiation." *Journal of the Nigerian Mathematical society* 35, no. 1 (2016): 245-256. https://doi.org/10.1016/j.jnnms.2016.02.006
[15] Jha, Basant K., B. Y. Isah, and I. J. Uwanta. "Combined effect of suction/injection on MHD free-convection flow in a vertical channel with thermal radiation." *Ain Shams Engineering Journal* 9, no. 4 (2018): 1069-1088. https://doi.org/10.1016/j.asej.2016.06.001
[16] Malik, Maulana, Mustafa Mamat, and Siti Sabariah Abas. "Convergence analysis of a new coefficient conjugate gradient method under exact line search." *International Journal of Advanced Science and Technology* 29, no. 5 (2020): 187-198.
[17] Abas, Siti Sabariah, and Yazariah Mohd Yatim. "Travelling-wave similarity solution for gravity-driven rivulet of a Newtonian fluid with strong surface-tension effect." In *AIP Conference Proceedings*, vol. 1870, no. 1, p. 040037. AIP Publishing LLC, 2017. https://doi.org/10.1063/1.4995869
[18] Malik, Maulana, Mustafa Mamat, Siti Sabariah Abas, and Ibrahim Mohammed Sulaiman. "A New Coefficient of the Conjugate Gradient Method with the Sufficient Descent Condition and Global Convergence Properties." *Engineering Letters* 28, no. 3 (2020).
[19] Alsagri, Ali Sulaiman, A. Hassanpour, and Abdulrahman A. Alrobaian. "Simulation of MHD nanofluid flow in existence of viscous dissipation by means of ADM." *Case Studies in Thermal Engineering* 14 (2019): 100494. https://doi.org/10.1016/j.csite.2019.100494
[20] Teh, Yuan Ying, and Adnan Ashgar. "Three dimensional MHD hybrid nanofluid Flow with rotating stretching/shrinking sheet and Joule heating." *CFD Letters* 13, no. 8 (2021): 1-19. https://doi.org/10.37934/cfdl.13.8.119
[21] Fekadu, Birlie, and H. V. Harish. "Numerical Studies on Thermo-Hydraulic Characteristics of Turbulent Flow in a Tube with a Regularly Spaced Dimple on Twisted Tape." *CFD Letters* 13, no. 8 (2021): 20-31. https://doi.org/10.37934/cfdl.13.8.2031

[22] Rusdi, Nadia Diana Mohd, Siti Suzilliana Putri Mohamed Isa, Norihan Md Arifin, and Norfifah Bachok. "Thermal Radiation in Nanofluid Penetrable Flow Bounded with Partial Slip Condition." *CFD Letters* 13, no. 8 (2021): 32-44. https://doi.org/10.37934/cfdl.13.8.3244
[23] Ebenezer Olubunmi, Ige, and Bidemi Olumide Falodun. "Incidence of Manifold Slip on Transport and Reaction Dynamics in Magneto-Bioconvective and Magnetic Nanoparticles Fe3O4 (Magnetite) Power-Law Flow Between Two Parallel Plates." *Journal of Nanofluids* 12, no. 1 (2023): 36-46. https://doi.org/10.1166/jon.2023.1907
[24] Falodun, B. O., and E. O. Ige. "Linear and quadratic multiple regressions analysis on magneto-thermal and chemical reactions on the Casson-Williamson nanofluids boundary layer flow under Soret-Dufour mechanism." *Arab Journal of Basic and Applied Sciences* 29, no. 1 (2022): 269-286. https://doi.org/10.1080/25765299.2022.2115688
[25] Latib, Muhammad Azamuddin, and Natrah Kamaruzaman. "Simulation Study on the Heat Performance of Different Nanofluids for Rotating Detonation Engine Cooling." *Journal of Advanced Research in Micro and Nano Engineering* 5, no. 1 (2021): 1-8.
[26] Mahat, Rahimah, Muhammad Saqib, Imran Ulah, Sharidan Shafie, and Sharena Mohamad Isa. "MHD Mixed Convection of Viscoelastic Nanofluid Flow due to Constant Heat Flux." *Journal of Advanced Research in Numerical Heat Transfer* 9, no. 1 (2022): 19-25.
[27] Sharafatmandjoor, Shervin. "Effect of Imposition of viscous and thermal forces on Dynamical Features of Swimming of a Microorganism in nanofluids." *Journal of Advanced Research in Micro and Nano Engineering* 8, no. 1 (2022): 1-8.
[28] Khan, Umair, William Pao, Nabihah Sallih, and Farruk Hassan. "Flow Regime Identification in Gas-Liquid Two-Phase Flow in Horizontal Pipe by Deep Learning." *Journal of Advanced Research in Applied Sciences and Engineering Technology* 27, no. 1 (2022): 86-91. https://doi.org/10.37934/araset.27.1.8691
[29] Omar, Nur Fatihah Mod, Husna Izzati Osman, Ahmad Qushairi Mohamad, Rahimah Jusoh, and Zulkhibri Ismail. "Analytical Solution on Performance of Unsteady Casson Fluid with Thermal Radiation and Chemical Reaction." *Journal of Advanced Research in Numerical Heat Transfer* 11, no. 1 (2022): 36-41.
[30] Idowu, A. S., and B. O. Falodun. "Variable thermal conductivity and viscosity effects on non-Newtonian fluids flow through a vertical porous plate under Soret-Dufour influence." *Mathematics and Computers in Simulation* 177 (2020): 358-384. https://doi.org/10.1016/j.matcom.2020.05.001
[31] Venkata Ramudu, A. C., K. Anantha Kumar, V. Sugunamma, and N. Sandeep. "Impact of Soret and Dufour on MHD Casson fluid flow past a stretching surface with convective–diffusive conditions." *Journal of Thermal Analysis and Calorimetry* (2022): 1-11. https://doi.org/10.1080/01430750.2022.2097947
[32] Fredrickson, Arnold Gerhard. *Principles and applications of rheology*. Prentice-Hall, 1964.